Corrections to Muonic X Rays and a Possible Proton Halo*

Roger C. Barrett†

Lawrence Radiation Laboratory, University of California, Berkeley, California

AND

Stanley J. Brodsky

Stanford Linear Accelerator Center, Stanford University, Stanford, California

AND

Glen W. Erickson

Crocker Nuclear Laboratory and Department of Physics, University of California, Davis, California

AND

Michael H. Goldhaber

Stanford Linear Accelerator Center and Department of Physics, Stanford University, Stanford, California

(Received 28 August 1967)

With the aim of extracting maximum information on nuclear charge structure at large distances, we improve the theory of muonic x rays in Bi^{209} by taking into account all known effects which could change the binding energy by as much as 0.1%. We give improved estimates of vacuum-polarization and Lamb-shift effects, and incorporate Cole's recent estimate of nuclear polarization effects. Using these corrections to analyze recent experiments on muonic x rays, we obtain parameters for the charge distribution in Bi^{209} which, when compared with parameters from electron scattering, indicate a small discrepancy. We suggest that this can be explained by a proton "halo," by which we mean a small fraction of the charge ($\sim$1%) spread over large distances ($\sim$8 F); we show that such a "halo" is not inconsistent with electron-proton scattering and brings the theory of the Lamb shift in atomic H and D into good agreement with experiments. We find no experiment with which such a model is inconsistent.

I. INTRODUCTION

MUONIC x rays and electron scattering provide alternative methods of investigating the electromagnetic structure of nuclei. Recently, measurements[1-3] have been made to high accuracy on heavy nuclei using both methods. This affords the possibility that careful analysis of muonic x rays may reveal structure at small momentum transfer not apparent from electron scattering results. To do this we must make sure that all corrections to muonic x rays not resulting from nuclear structure are properly taken into account. We shall, in particular, try to understand corrections of order 0.1% (a few keV) to the muonic x-ray spectrum of a spherical nucleus, Bi^{209}.

In Sec. II, we give improved estimates of vacuum-polarization and Lamb-shift corrections to muonic energy levels. For the vacuum-polarization contribution, we extend the asymptotic formula and give a careful estimate of its validity. For the Lamb shift, we find that many previous estimates are not valid, and we obtain results, to about 40% accuracy, which are larger than Hill and Ford's order-of-magnitude estimate of 1 keV or less.[4]

Of the other effects we discuss in Sec. II, the most important is nuclear polarization, which has recently been treated carefully by Pieper and Greiner[5] and by Cole.[6] Other energy shifts due to nuclear multipole moments, electron screening, nuclear motion, and "granularity" are discussed and estimated to be small.

In Sec. III, we give parameters for the charge distribution of Bi^{209} which we have calculated from recent experiments on muonic x rays, and compare these with similar parameters obtained by electron scattering. We find a discrepancy larger than one standard deviation.

In Sec. IV, we suggest a tantalizing explanation for this discrepancy in terms of a proton tail or "halo," by which we mean a small fraction of the charge spread out over an anomalously large distance[7] of the order of 10 F. We point out that such a halo could also explain the present small discrepancy between theory and experiment for the Lamb shifts in atomic hydrogen and deuterium. We also show that such a halo is not in disagreement with other experiments which might be expected to detect it. In fact, the electron-proton scattering data at low momentum transfer apparently indicate the presence of such a

---

* Supported in part by the U. S. Atomic Energy Commission.
† Present address: University of Surrey, England.
¹ T. T. Bardin, R. C. Cohen, S. Devons, D. Hitlin, E. Macagno, J. Rainwater, K. Runge, C. S. Wu, and R. C. Barrett, Phys. Rev. **160**, 1043 (1967).
² G. J. C. van Niftrik and R. Engfer, Phys. Letters **22**, 490 (1966).
³ H. Anderson, in Proceedings of the International Conference on Electromagnetic Sizes of Nuclei, Ottawa, 1967 (to be published).
⁴ D. L. Hill and K. W. Ford, Phys. Rev. **94**, 1617 (1954). Erroneous estimates of the Lamb shift in muonic atoms have

been given by A. B. Michelwait and N. C. Corben, Phys. Rev. **96**, 1145 (1954). Also, see references listed in footnote 1 of this paper and Ref. 9.
⁵ W. Pieper and W. Greiner, Phys. Letters **24B**, 377 (1967).
⁶ R. K. Cole, Jr., Phys. Letters **25B**, 178 (1967).
⁷ This possibility has also been considered by W. E. Lamb, Jr. (private communication to G. W. E.). Our ideas evolved from a suggestion by Professor T. D. Lee that an anomalous behavior of the proton form factors at small momentum transfer could be responsible for the (then present) hyperfine splitting discrepancy in hydrogen (private communication to S. J. B.).

charge distribution; the usual assumption that the proton charge form factor is essentially a linear function of momentum transfer squared (q^2) for $q^2 < m_\pi^2$ has not been demonstrated experimentally. A similar halo model for the neutron can also account for the known features of the neutron charge form factor.

II. THEORY AND CORRECTIONS TO MUONIC X RAYS

The basic theory of muonic energy levels for Bi[209] consists of the Dirac equation for a muon (with reduced mass) in the static spherical charge distribution of the nucleus. Corrections to this theory are discussed below. The charge distribution parametrization is discussed in Sec. III. The Dirac Hamiltonian includes the vacuum-polarization potential due to free electron-positron pairs as given in Eq. (2.2). The results of this paper are obtained by finding a best fit of the nuclear parameters to the observed x-ray spectrum.[1] The Dirac equation was solved numerically.[8]

Before we can confidently compare the obtained bismuth charge distribution with that given by the analysis of electron scattering, we must make sure all corrections to muonic x rays not resulting from nuclear structure are correctly taken into account. Our discussion of neglected contributions is meant to complement and bring up to date previous treatments of Pustovalov,[9] and Hill and Ford.[4] We will attempt to include all corrections which affect the energy levels to 0.1%.

The differences between the above theory and an exact treatment of bismuth muonic x rays as given by quantum electrodynamics and nuclear physics are the following.

(a) *Finite nuclear mass.* The nuclear motion is nearly entirely taken into account by using the reduced mass in the Dirac equation. The residual contribution not accounted for by this prescription is expected to be of the order of

$$-\frac{(Z\alpha)^4}{8n^4}\frac{m}{M}m, \qquad (2.1)$$

the contribution[10] for a point nucleus. The nuclear motion must also be taken into account in the definition of the nuclear charge form factor. These corrections are less than 10^{-4} of the binding energy and are neglected.

(b) *Nonspherical components of the charge distribution.* The Bi[209] nucleus is very nearly spherical (consisting of one proton added to a doubly-magic core). We assume that the effects of nuclear deformation and the discrete charge distribution of protons in the nucleus

(granularity) contribute similarly to the charge distribution obtained from the unpolarized electron elastic scattering differential cross section and to the charge distribution obtained by fitting muon x-ray fine structure.

(c) *Nuclear polarization.* There have been two recent attempts to estimate the contribution of nuclear polarization to muonic levels using specific models. Cole[6] has calculated the effect of the giant dipole resonance and finds the binding of the $1S$, $2P_{1/2}$, $2P_{3/2}$, and $3D$ states to be increased by 4.6, 1.6, 1.4, and 0.1 keV, respectively, in bismuth. Cole considers this to be a *lower bound*; the actual nuclear polarization will probably be within a factor of 2 of these values when other intermediate states are included. Pieper and Greiner[5] have performed a similar calculation, but which includes all multipole excitations, and obtain somewhat smaller results for Bi[209].

To a certain extent, nuclear polarization is also contained in the electron scattering form factors; detailed calculations have not been made to our knowledge.

(d) *Electron screening.* The effect of the atomic electrons on the muon energy levels in Bi[209] has been calculated. The electron density was taken to be that obtained in a relativistic self-consistent calculation[11] for Hg, modified by a factor $(Z/80)^3$. The potential due to the electrons is of the form $a - br^{2\sigma}$, where $\sigma = (1 - \alpha^2 Z^2)^{1/2}$ (a, $b > 0$). Thus the screening reduces the transition energies. We ignore the constant term a which has the effect of raising all the levels by a constant amount (several keV in magnitude). The effect of the second term is very nearly proportional to $(3n^2 - l^2 - l)^{2\sigma}$ except for the lowest muon levels, and varies from 4.6 eV for the $1S$ state to 190 eV for the $5G$ states. Thus the screening effect can be ignored for the transitions in which we are interested.

(e) *Vacuum polarization.* For a spherically symmetric charge distribution $\rho(r)$, the vacuum polarization potential due to virtual free electron-positron pairs is[12]

$$V_{vp}(r) = \frac{4\alpha}{3\pi} \int_0^\infty dr' \frac{r'}{r}[H(|r-r'|) - H(r+r')]\rho(r') \quad (2.2)$$

with

$$H(r) = \frac{1}{2}\lambda_e \int_1^\infty \frac{dy}{y^2} \exp(-2yr/\lambda_e)\left(1+\frac{1}{2y^2}\right)\left(1-\frac{1}{y^2}\right)^{1/2}, \qquad (2.3)$$

where $\lambda_e = 1/m_e \simeq 386$ F is the reduced Compton wavelength of the electron. The asymptotic expansion of

[8] R. C. Barrett (to be published) and S. Cohen, Phys. Rev. **118**, 489 (1960).

[9] G. E. Pustovalov, Zh. Eksperim. i Teor. Fiz. **32**, 1519 (1957) [English transl.: Soviet Phys.—JETP **5**, 1234 (1957)].

[10] H. A. Bethe and E. E. Salpeter, *Quantum Mechanics of One- and Two-Electron Atoms* (Academic Press Inc., New York, 1957), Eq. (42.7).

[11] S. Cohen, University of California Radiation Laboratory Report No. UCRL-8389, 1958 (unpublished).

[12] K. W. Ford and J. G. Wills, Nucl. Phys. **35**, 295 (1962).

$H(r)$ for $r \ll \lambda_e$ is

$$H(r)-H(0)=r\left\{\ln\left(\frac{r\gamma}{\lambda_e}\right)-\frac{1}{6}-\frac{3\pi}{8}\frac{r}{\lambda_e}+\frac{1}{2}\left(\frac{r}{\lambda_e}\right)^2-\frac{\pi}{12}\left(\frac{r}{\lambda_e}\right)^3\right.$$

$$\left.+O\left[\left(\frac{r}{\lambda_e}\right)^4\ln\left(\frac{r}{\lambda_e}\right)\right]\right\}, \quad (2.4)$$

where $\ln\gamma = 0.557^+$ is Euler's constant. We have carried out calculations using both the exact form [Eq. (2.3)] and the asymptotic expansion. The first two terms in Eq. (2.4) which were used in previous calculations,[12,13] give $H(r)$ to an accuracy of 2% for $r \lesssim 50$ F; the terms through order $(r/\lambda_e)^3$ are needed to yield the same accuracy up to $r \lesssim 180$ F and have been included in our analysis of the muon spectra. Higher-order iterations of this second-order vacuum-polarization potential have been taken into account by including $V_{\rm vp}$ in the Dirac Hamiltonian. The effect of the vacuum-polarization potential due to muon pairs has been included with the Lamb shift as the $-\frac{1}{5}$ in Eq. (2.5), where we find the contribution to be small. Vacuum polarization due to hadron pairs is implicitly included in the nuclear form factor.

We have not included the fourth-order vacuum-polarization potential,[14] a correction of relative order $\alpha/\pi \cong 1/500$. We have also ignored the influence of the nuclear charge distribution on the virtual electron pairs. Wichmann and Kroll[15] have shown that this correction is negligible ($\sim 2\times10^{-4}$ times the muon binding energy) even for uranium with a point charge distribution.

(*f*) *Other radiative corrections of order* α. Previous estimates of the Lamb shift in muonic atoms have used the invalid argument that this contribution is *a priori* of order m_e^2/m_μ^2 smaller than that of electron-pair vacuum polarization. Actually the vacuum-polarization potential has the assumed $1/m_e^2$ dependence only for $r \gg \lambda_e$; the important region for muonic atoms is instead $r \ll \lambda_e \simeq 386$ F in which case the m_e dependence in Eq. (2.4) is logarithmic. In fact, the Lamb shift would be comparable[16] to the electron-pair vacuum-polarization contribution in heavy muonic atoms if the nucleus were a point charge, and turns out to be smaller only because the potential is not singular at small distances.

The usual $Z\alpha$ expansion of the Lamb-shift expression might be expected to fail for muonic bismuth, with $Z\alpha \simeq 0.6$, but we find in Appendix A that the field

strength expansion[17] is adequate (to 30% accuracy) for the low-lying states because the muon does not see a singular Coulomb potential. We may thus use the usual lowest-order formula[17]

$$\Delta E_{\rm LS}=\frac{\alpha}{3\pi m^2}\langle\nabla^2 V\rangle\left[\ln\frac{m}{2\Delta\epsilon}+\frac{11}{24}+\frac{3}{8}-\frac{1}{5}\right]$$

$$+\frac{\alpha}{8\pi m^2}\left\langle\frac{2}{r}\frac{dV}{dr}\boldsymbol{\sigma}\cdot\mathbf{L}\right\rangle, \quad (2.5)$$

where $\Delta\epsilon$ is the average excitation energy defined by the Bethe sum. As shown in Appendix A, it is sufficient to our accuracy to approximate $\Delta\epsilon_n$ by the binding energy of the state. The $(-\frac{1}{5})$ term corresponds to the vacuum polarization of muon pairs. The $\frac{3}{8}$ and the spin-orbit term correspond to the muon anomalous magnetic moment.

Here

$$\langle\nabla^2 V\rangle=4\pi Z\alpha\langle\rho\rangle \quad (2.6)$$

is proportional to the probability of overlap of the muon wave function with the nuclear charge distribution. We note that we now have a non-negligible Lamb shift for the $2P$ states since the overlap is $\sim 10\%$ in contrast to the vanishing overlap with point nuclei. The expectation values in Eq. (2.5) have been evaluated numerically (and are tabulated in Appendix A) and we find

$$\begin{aligned}\Delta E_{\rm LS}=\quad &3.0 \pm 1.0 \quad \text{keV}, \quad 1S\\ =\quad &0.4 \pm 0.3 \quad \text{keV}, \quad 2P_{1/2}\\ =\quad &0.7 \pm 0.3 \quad \text{keV}, \quad 2P_{3/2}\\ =\quad &{-}0.04\pm0.02\ \text{keV}, \quad 3D_{3/2}. \quad (2.7)\end{aligned}$$

The error limits here are due primarily to the uncertainty in the value of the Bethe logarithm in Eq. (2.5).

III. NUCLEAR CHARGE DISTRIBUTION

The most frequently used parametrization of the radial distribution of nuclear charge is the Fermi shape

$$\rho(r) \propto 1/[1+e^{(r-c)/a}], \quad (3.1)$$

where c is the half-density radius and $t \equiv (2\ln9)a$ is the 90–10% fall-off distance. We follow this somewhat arbitrary choice for convenience, although there are a wide variety of two-parameter distributions which can be adjusted to fit experimental measurements. In the case of muonic atoms, the K and L x-ray transitions enable us to determine only the lowest moments—$\int d^3r\,\rho(r)r^2$ and $\int d^3r\,\rho(r)r^4$—and little else. In principle, higher moments of the charge distribution would be given by higher transitions but these are very close to the point-charge values and the volume shift is no more than one

[13] H. L. Acker, G. Backenstoss, C. Gaum, J. C. Sens, and S. A. De Wit, Nucl. Phys. **87**, 1 (1966).

[14] M. Baranger, F. J. Dyson, and E. E. Salpeter, Phys. Rev. **88**, 680 (1952).

[15] E. H. Wichmann and N. M. Kroll, Phys. Rev. **101**, 843 (1956).

[16] We find a Lamb shift of ~100 keV in the $1S$ state of muonic bismuth with a point charge by using $m \to m_\mu$ and $Z=83$ in the point-charge results of D. F. Mayers, G. E. Brown, and E. A. Sanderson, Phys. Rev. Letters **3**, 90 (1959).

[17] R. Karplus, A. Klein, and J. Schwinger, Phys. Rev. **86**, 288 (1952); G. W. Erickson and D. R. Yennie, Ann. Phys. (N. Y.) **35**, 271 (1965); **35**, 447 (1965).

TABLE I. Muonic x-ray energies in Bi^{209} (in keV). The experimental energies are from Bardin *et al.* (Ref. 1). The next two columns show the theoretical fit to the energies for c and t as given in Sec. III. The corrected theory takes into account the muonic Lamb shift and a nuclear polarization estimate. The last column gives the energies predicted from the electron scattering parameters of Ref. (19). [These predictions may be misleading since a change in c of 0.02 F would bring the K x rays into agreement with experiment. There would still be a discrepancy of about 3 keV in the L x rays, however.]

Transition	Experiment	Theory (uncorrected)	Theory (corrected)	Prediction from electron scattering
$2P_{1/2}-1S$	5841.5 ± 3.0	5842.0	5841.8	5854.6
$2P_{3/2}-1S$	6032.4 ± 3.0	6032.2	6032.3	6046.0
$3D_{3/2}-2P_{1/2}$	2699.5 ± 1.0	2698.8	2699.0	2704.8
$3D_{5/2}-2P_{3/2}$	2552.8 ± 1.0	2553.5	2553.3	2558.2
$4F_{5/2}-3D_{3/2}$	996.6 ± 1.0	996.6	996.7	996.8
$4F-3D_{5/2}$	961.8 ± 1.0	961.1	961.2	961.2
$5G-4F$	444.5 ± 1.0	444.9	445.0	445.0

order of magnitude larger than the experimental errors. This restriction to lower moments can also be seen in the expansion of the Fourier transform of the charge distribution,

$$f(q^2) \equiv \int d^3r\, e^{i\mathbf{q}\cdot\mathbf{r}}\rho(r)$$

$$= 1 - q^2\frac{\langle r^2\rangle}{6} + q^4\frac{\langle r^4\rangle}{120} - \cdots + (-1)^n q^{2n}\frac{\langle r^{2n}\rangle}{(2n+1)!} + \cdots,$$

in which the expansion coefficients are the moments divided by increasingly large numbers. Since the finite nucleus, with $\langle r^{2n}\rangle \cong R^{2n}$, restricts bound-state momenta to $q<1/R$, it is apparent that the higher terms are seen only in scattering experiments with $q>1/R$ or in precise bound-state experiments.

We have carried out calculations of muonic x-ray transition energies in order to compare our results with those from low-energy electron scattering experiments. The results of a recent measurement[1] of the muonic spectrum of Bi^{209} are shown in Table I. If none of the corrections discussed in Sec. II are included, the Fermi shape parameters which correspond to this spectrum are $c=6.66\pm0.04$ F, $t=2.32\pm0.10$ F. If we take into account the Lamb shifts of Eq. (2.7) and Cole's lower bound[6] of the polarization of the nucleus by the muon, we obtain $c=6.63\pm0.03$ F, $t=2.40\pm0.08$ F.[18] The t parameter is *increased* even further if the nuclear polarization is increased further.

The analysis[19] of a recent 50-MeV electron scattering experiment[2] on Bi^{209} gives the results $c=6.74\pm0.08$ F, $t=2.00\pm0.16$ F.

We have also analyzed the charge distribution for Pb^{208} using recent accurate muon x-ray measurements[3] and have compared the shape with that obtained from electron scattering on natural lead.[2] The muon results again indicate a larger tail for the nucleus.[20]

The discrepancy between the muonic x ray and electron scattering results may be due to the arbitrary choice of the Fermi shape for the charge distribution. The electron scattering results are insensitive to variations in the tail of the charge distribution, while muonic levels are very sensitive to such changes. The tail of the Fermi shape, $e^{-r/a}$, falls off more slowly than the results of nuclear matter calculations or single-particle shell-model calculations.[21,22] However, if we use a shape with a shorter tail, we find a larger discrepancy. (If a parametrization yielding a larger $\langle r^2\rangle^{1/2}$ and $\langle r^4\rangle^{1/4}$ should be used, this in itself might be a consequence of the proton halo proposed in the next section.)

It should be noted that the analysis of the electron experiments, which are based on a partial wave expansion, have not yet taken nuclear polarization (dispersion corrections) into account. At 300 MeV, $\theta=5°$, positron scattering on Bi^{209} shows a 2.2 standard deviation discrepancy with the no-polarization partial-wave predictions.[23]

IV. PROTON HALO

The disagreement between the nuclear charge distributions obtained from muonic x rays and electron scattering may be a significant discrepancy and should warrant a careful investigation of possible corrections such as the effect of nuclear polarization and higher-order radiative corrections in the electron scattering analysis. On the other hand, the bound muon interacts at small q^2 and may well be observing a long charge tail on the nucleus; the results given in this section show that satisfactory fits to the muon x rays are obtained by combining a charge tail with the Fermi charge distribution obtained from electron scattering.

[18] The corresponding moments of the bismuth charge distribution are $\langle r^2\rangle^{1/2}=5.52$ F, $\langle r^4\rangle^{1/4}=5.87$ F ($\chi^2=1.5$) for the "uncorrected" spectrum, and $\langle r^2\rangle^{1/2}=5.52$ F, $\langle r^4\rangle^{1/4}=5.89$ F ($\chi^2=0.9$) when the muonic Lamb shift and nuclear polarization are included.

[19] G. J. C. van Niftrik (preliminary result, to be published) (private communication from R. Engfer). The corresponding moments are $\langle r^2\rangle^{1/2}=5.49$ F, $\langle r^4\rangle^{1/4}=5.81$ F.

[20] Discrepancies between muonic x rays and electron scattering in heavy nuclei have also been noted by L. R. B. Elton, in Proceedings of the International Conference on Electromagnetic Sizes of Nuclei, Ottawa, 1967 (to be published); and D. G. Ravenhall (unpublished). The electron scattering data and muonic x rays can be reconciled by introducing an additional shape parameter, perhaps in the form of a factor $(1+\alpha r^2)$ multiplying Eq. (3.1), with $\alpha>0$. This increases the tail of the charge distribution for a given c and t. We wish to thank Dr. D. G. Ravenhall for informing us of his work with B. C. Clark and R. Hermann concerning such three-parameter shapes. We shall suggest a more radical modification of the charge distribution in Sec. IV.

[21] H. A. Bethe, in *Proceedings of the International Conference on Nuclear Physics, Gatlinburg, 1966* (Academic Press Inc., New York, 1967); Bull. Am. Phys. Soc. **12**, 83 (1967).

[22] L. R. B. Elton, in Proceedings of the Williamsburg Conference on Intermediate Energy Physics, 1966, p. 48 (unpublished).

[23] J. Goldemberg, J. Pine, and D. Yount, Phys. Rev. **132**, 406 (1963); A. Browman, B. Grossetête, and D. Yount, *ibid.* **143**, 899 (1966). T. de Forest and J. D. Walecka [Advan. Phys. **15**, 1 (1966)] review the theoretical treatment of the dispersion corrections.

TABLE II. Lamb-shift comparisons (MHz).

	Theory[a]	Experiment[bc]	Discrepancy	Increase of theory for tripled $\langle r^2 \rangle_{\text{proton}}$
H	1057.56 ± 0.08	R 1057.86 ± 0.10	0.30 ± 0.18	0.25
		L 1057.77 ± 0.10	0.21 ± 0.18	0.25
D	1058.82 ± 0.14	R 1059.19 ± 0.10	0.37 ± 0.24	0.25
		L 1059.00 ± 0.10	0.18 ± 0.24	0.25
He$^+$	$14\,040.0\ \pm4.0$	$14\,040.2\ \pm4.5$	$0.2\ \pm8.5$	4.1
He$^+(n=3)$	$4182.7\ \pm1.2$	$4182.5\ \pm14$	$-0.2\ \pm15$	1.2
He$^+(n=4)$	$1768.4\ \pm0.5$	$1766.0\ \pm7.5$	$-2.4\ \pm8.0$	0.5
Li^{++}	$62\,743\pm43$	$63\,031\pm327$	288 ± 370	21

[a] See Ref. 27.
[b] In this column, the letters R and L refer to Refs. 24 and 25, respectively.
[c] The errors in this column are $\sim$3 standard deviations.

It is interesting to speculate, however, that this charge tail may be due to an anomalous charge distribution on the *proton* which we call the proton halo and shall now describe.[7]

To motivate our introduction of this "halo" we turn our attention to quite a different realm of atomic structure: the Lamb shift, not in heavy muonic atoms, but in ordinary atomic hydrogen and deuterium. The most recent theoretical and experimental numbers are given in Table II. These include the "e/h" value of α in the theory, and Robiscoe's corrected version[24] of his and Cosens's measurements, which are now in essential agreement with the results of Lamb et al.[25] As shown in the third column, there remains a discrepancy larger than the sum of the estimated limits of error of both theory and experiment (*more than three standard deviations*); this discrepancy is about the same for both H and D[26]: theory is about $\frac{1}{4}$ MHz below experiment.

Now, the effect of the finite nuclear size on the Lamb shift is given by[27]

$$\delta E_{\text{LS}} = \frac{4Z^4 \text{Ry}}{3n^3} \frac{\langle r^2 \rangle}{a_0^2}, \qquad (4.1)$$

where r is the charge radius of the proton and a_0 is the Bohr radius of the atom. If we assume, as usual, that the proton has a root-mean-square (rms) charge radius of 0.8 F$\equiv R_0$ we find that this term contributes 0.12 MHz to the Lamb shift in H. W could explain the discrepancy if, instead of taking the usual value, we assumed that $\langle r^2 \rangle$ were much larger. This would be the case if the proton had a "halo," by which we mean that a small fraction ϵ of its charge would be distributed over a distance much larger than R_0. For a proton having a halo with rms radius $R_H \gg R_0$ and a reduced body with rms radius $R_b \cong R_0$, the mean square radius is

$$\langle r^2 \rangle_{\text{new}} = (1-\epsilon)R_b^2 + \epsilon R_H^2. \qquad (4.2)$$

The Lamb-shift contribution of Eq. (4.1) would be tripled (yielding the desired increase of $\frac{1}{4}$ MHz in H and D) if $\langle r^2 \rangle_{\text{new}} = 3R_0^2$ or

$$\epsilon R_H^2 = 3R_0^2 - (1-\epsilon)R_b^2 \cong 2R_0^2. \qquad (4.3)$$

This can be achieved with any value of ϵ and an appropriate choice of R_H. Figure 2 will show ϵ as a function of R_H for $R_b = R_0$ and for $R_b = 0.9R_0$.

On the other hand, the effect of the finite nuclear size on the hyperfine splitting of the $1S$ state is approximately given by[28]

$$\delta E_{\text{hfs}} = -2\frac{\langle r \rangle}{a_0}E_{\text{hfs}}. \qquad (4.4)$$

For the usual proton charge distribution this is -30 parts per million (ppm) of the total splitting (E_{hfs}) in hydrogen. If the proton halo has the same shape as (but larger size than) the usual distribution, then the hfs contribution is changed by the factor

$$\frac{\langle r \rangle_{\text{new}}}{\langle r \rangle_0} = (1-\epsilon)\frac{\langle r \rangle_b}{\langle r \rangle_0} + \epsilon\frac{\langle r \rangle_H}{\langle r \rangle_0} \cong 1 + \epsilon R_H/R_0, \qquad (4.5)$$

assuming the reduced body also has the same shape as the usual distribution. Since there is room only for about 10 ppm error in the hfs theory,[29] then we must have

$$\epsilon R_H/R_0 \lesssim \frac{1}{3}. \qquad (4.6)$$

By combining this with Eq. (4.3), and assuming for simplicity $R_H > R_b$ and $\epsilon \ll 1$, we find the approximate restrictions

$$\epsilon \lesssim 1/18 \cong 6\% \quad \text{and} \quad R_H \gtrsim 6R_0 \cong 5\,\text{F}, \qquad (4.7)$$

if we are to have the desired Lamb-shift increase without disturbing the hfs agreement. Taking $R_b < R_0$ and

[24] R. T. Robiscoe, Phys. Rev. (to be published); S. J. Brodsky and R. G. Parsons, *ibid.* **163**, 134 (1967).

[25] S. Triebwasser, E. S. Dayhoff, and W. E. Lamb, Jr., Phys. Rev. **89**, 98 (1953).

[26] The discrepancy is further increased by 0.06 MHz if the value of α from the fine-structure measurements is used.

[27] Equation (4.10b), Erickson and Yennie, Ref. 17.

[28] Because the hfs contribution is not found to be an important limitation on a proton halo, we have only used the simple coordinate-space form (4.4) given by A. C. Zemach, Phys. Rev. **104**, 1771 (1956), Eq. (2.10). See also F. Guerin, Ph.D. thesis, University of Paris (Orsay), 1966 (unpublished); D. R. Yennie and W. Grotch; (to be published); and Ref. 29 for recent treatments of the proton corrections to the hyperfine structure. The radiative corrections are summarized in S. J. Brodsky and G. W. Erickson, Phys. Rev. **148**, 26 (1966).

[29] S. D. Drell and J. D. Sullivan, Phys. Rev. **154**, 1477 (1967).

$$\frac{R^2}{6} = 3 \times \frac{R_0^2}{6}$$

(a) $R_H = 6F$, $\epsilon = 3.7\%$
(b) $R_H = 10F$, $\epsilon = 1.3\%$
(c) $R_H = 16F$, $\epsilon = 0.5\%$
(d) USUAL FIT: $\epsilon = 0$

$$G_{Ep} = \frac{1-\epsilon}{\left[1+q^2\frac{R_0^2}{12}\right]^2} + \frac{\epsilon}{\left[1+q^2\frac{R_H^2}{12}\right]^2}$$

$R_0 = 0.8$ F
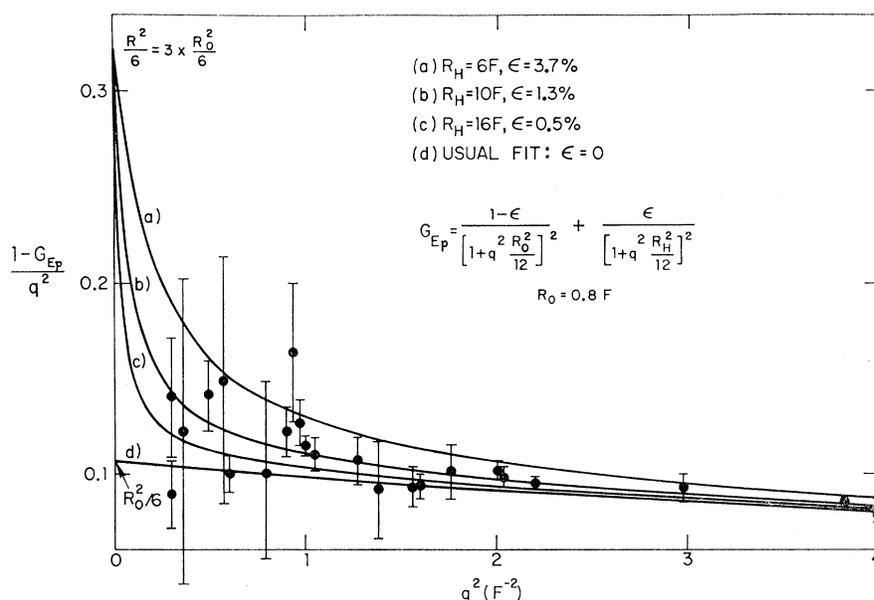
FIG. 1. The slope function of the proton charge form factor $(1-G_{Ep})/q^2$ (in F^2). The three upper curves show the effect of a proton halo of charge $\epsilon|e|$ and rms radius R_H. The total proton rms radius is taken to be tripled in order to fit the Lamb shift in H. The usual fit to G_{Ep} for small q^2 corresponds to $\epsilon = 0$. The data are taken from Ref. 30.

treating Eqs. (4.3) and (4.6) exactly would somewhat weaken the restrictions, but would overcomplicate the analysis at this point; these refinements are included in Fig. 2, where it will be seen that the hfs is not an important limitation.

For different restrictions on a proton halo, let us next consider the elastic scattering of electrons from protons, which more or less directly measures the electric form factor of the proton, $G_{Ep}(q^2)$, the Fourier transform of the proton charge distribution. The derivative at the origin, $G'(0) = -\langle r^2\rangle/6$, is proportional to the mean square radius of the charge distribution, so the measurements at small q^2 may be expected to limit severely the size of the proton halo. A glance at a plot of G versus q^2, with the points all approaching $G(0) = 1$ in an apparently straight line near $q^2 = 0$, would seem to rule out the existence of a halo. However, the approach to $G(0) = 1$ only verifies the charge of the proton, and the slope of the straight line only gives the approximate radius of the body. If the halo has R_H large enough that its form factor is negligible at the observed values of q^2, then we could obtain a bound on ϵ by fitting a smooth form factor to the data and extrapolating back to $G_b(0) = 1 - \epsilon$. For a smaller R_H, however, the halo and the body both contribute, and the curvature of the form factor must be taken into account.

To see more clearly the behavior of the form factors at small q^2, let us plot $(1-G)/q^2$ versus q^2, as in Fig. 1, using the data given by Wilson and Levinger and others.[30] The usual analysis fits a straight line

$$\frac{1-G}{q^2} = \frac{\langle r^2\rangle_0}{6} - q^2\frac{\langle r^4\rangle_0}{120} \tag{4.8}$$

to these data at small q^2. A halo raises the $q^2 \simeq 0$ end of the curve, and the value at $q^2 = 0$ gives the *total* mean square radius, $\langle r^2\rangle/6$. For very large R_H (and small ϵ), the curve drops sharply from $\langle r^2\rangle/6$ and the halo contribution is negligible at the smallest observed values of q^2; the linear fit to the data then gives the size of the corresponding reduced body of the proton. For smaller R_H, the halo will start raising the curve at observed values of q^2; such a trend is actually present in the data if we ignore data at $q^2 = 0.3$ F^{-2}. The curves show $(1-G)/q^2$ for halos of various sizes which give a $\frac{1}{4}$ MHz Lamb-shift increase; the (approximately) straight line is for no halo.

In Appendix B we discuss the quantitative limits of the halo due to electron-proton scattering. The findings are summarized in Fig. 2. It is found that for $R_H \gtrsim 8$ F, halos are allowed which are consistent with the hfs agreement and an increase in the Lamb shift of $\gtrsim 0.15$ MHz. At the least, one can conclude that the usual assumption that the proton form factor is a linear function of q^2 for $q^2 < m_\pi^2$ has not been experimentally demonstrated.

Since the e-p scattering does not restrict the Lamb-shift contribution of a halo with $R_H > 10$ F, we now seek a halo effect that will provide a stronger limit at large R_H than a bound on ϵR_H^2. Here we return to

[30] D. Frèrejacque, D. Benaksas, and D. Drickey, Phys. Rev. **141**, 1308 (1966); T. Janssens, R. Hofstadter, E. B. Hughes, and M. R. Yearian, *ibid.* **142**, 922 (1966); R. R. Wilson and J. S. Levinger, Ann. Rev. Nucl. Sci. **14**, 135 (1964), and previous work cited therein, excluding the values from D. Yount and J. Pine, Phys. Rev. **128**, 1842 (1962), which have been normalized to $G(0) = 1$. The data have not been corrected for second Born contributions. From the positron-proton results of Yount and Pine we estimate that the correction of this omission would raise the data points in Fig. 1 by 0.008 for the lowest values of q^2 and less than this for the other points. These changes would enhance the indication of a halo, but in any event, are smaller than the error limits given. We wish to thank Dr. F. Von Hippel for discussions on this point.

FIG. 2. Restrictions on the proton halo: allowed percentage versus rms radius. Upper limits are given by the hyperfine structure (hfs) in the ground state of H and elastic electron-proton (e-p) scattering using Eqs. (B1–B3). The curves labeled LS show the halo required to fit the 0.25-MHz Lamb-shift discrepancy in hydrogen. In each case the lower curve corresponds to $R_b = R_0 \simeq 0.8$ F and the upper curve to $R_b = 0.9 R_0 \simeq 0.7$ F. The Bi curves give the range of halo parameters needed to reconcile the Bi^{209} charge distributions obtained in electron-bismuth scattering with our results from muonic x rays.
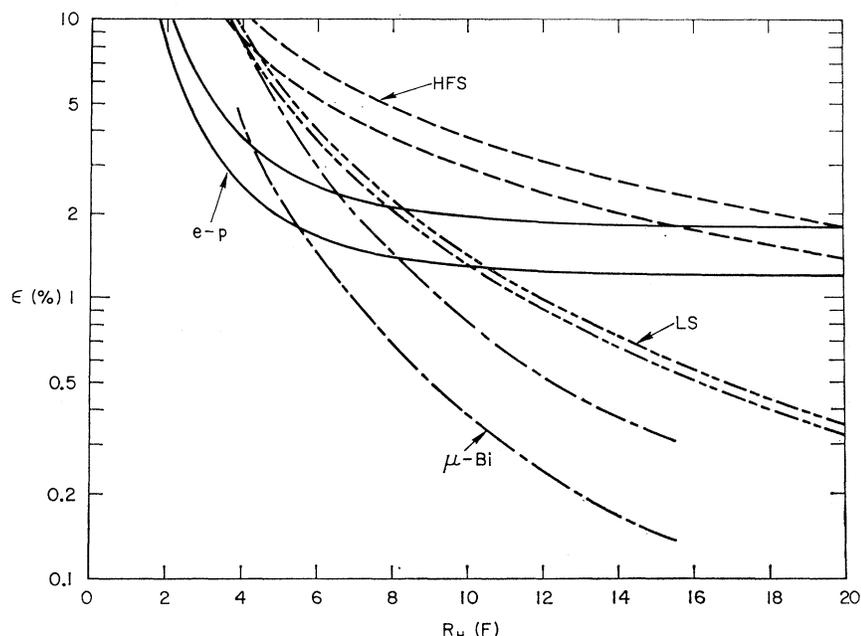
muonic x rays, which have some dependence on the fourth moment of the nuclear charge distribution and thus will eventually provide a bound on ϵR_H^4 for large enough R_H. As seen in Fig. 2, the muonic x rays in Bi indeed provide such a bound (and provide a stronger restriction than e-p scattering for halos with $R_H \gtrsim 8$ F), and moreover are found to give results consistent with e-Bi scattering if we include a halo with ϵ between the two Bi curves in Fig. 2.

In Sec. III we have given the Fermi shape parameters c and t resulting from a least-squares adjustment to the experimental muon x-ray spectrum of Bi^{209}. We now consider the effect of introducing a proton halo as described above. Folding protons with mean square radius

$$\langle r^2 \rangle_p = (1 - \epsilon) \langle r^2 \rangle_b + \epsilon \langle r^2 \rangle_H$$

into a nucleus with proton centers distributed with mean square radius $\langle r^2 \rangle_C$ yields a nuclear charge distribution with mean square radius

$$\langle r^2 \rangle_N = \langle r^2 \rangle_C + \langle r^2 \rangle_p$$
$$= (1 - \epsilon)[\langle r^2 \rangle_C + \langle r^2 \rangle_b] + \epsilon[\langle r^2 \rangle_H + \langle r^2 \rangle_N]. \quad (4.9)$$

We obtain the total nuclear charge density by adding a Fermi shape of reduced charge $(1 - \epsilon)Ze$ to a tail of charge ϵZe with a shape obtained by folding a uniform

TABLE III. Parameters of bismuth charge distribution with halo.

$(5/3)^{1/2} R_H$ (F)	ϵ (%)	c (F)	$\langle r^2 \rangle^{1/2}$ (F)	$\langle r^4 \rangle^{1/4}$ (F)	χ^2
5	7.0±2.8	6.68±0.03	5.524	5.891	0.90
7	2.9±1.2	6.67±0.02	5.525	5.903	0.92
10	1.1±0.5	6.68±0.01	5.528	5.926	0.94
14	0.5±0.2	6.69±0.01	5.531	5.964	1.00
20	0.2±0.1	6.70±0.01	5.539	6.058	1.21

proton halo of radius $(5/3)^{1/2} R_H$ into a uniform sphere of radius c. The fits to the x-ray data were obtained for fixed values of R_H and t by varying ϵ and c. The values of t were taken to be the upper and lower limits given by $e - Bi^{209}$ scattering.[2] The results for both limits are shown in Fig. 2. Table III lists the average of these two limits, with an error interval given by the rms sum of half this difference and the additional difference that would double the value of χ^2. The results take into account the corrections for the Lamb shift and Cole's estimate of the nuclear polarization. It might be noted that the values of χ^2 increase as R_H increases, indicating that larger halos should be restricted more than the indicated trend of the Bi curves in Fig. 2, probably more like a bound on ϵR_H^4.

The above modification of nuclear charge distribution may be expected to have effects only of relative order $\epsilon \sim 1\%$ in e-Bi scattering. A more precise analysis would determine the various scattering corrections to this accuracy and simultaneously fit μ-Bi x rays and e-Bi scattering, but we expect the final result to agree with the present analysis.

Our conclusions on the presence of a halo on the bismuth nucleus would be changed if nuclear polarization or other corrections turn out to be important in the analysis of electron-bismuth scattering.

Let us note in passing that the measured neutron form factor could also be easily interpreted in terms of a halo of the same size and shape as the proton halo. For zero charge we write

$$G_{En}(q^2) = -\epsilon_n G_b(q^2) + \epsilon_n G_H(q^2). \quad (4.10)$$

The slope at $q^2 = 0$,[31]

$$-\tfrac{1}{6} \langle r^2 \rangle_n = G_{En}'(0) = 0.021 \ F^2 \simeq \tfrac{1}{5}(R_0^2/6), \quad (4.11)$$

[31] V. E. Krohn and G. R. Ringo, Phys. Rev. 148, 1303 (1966), and references contained therein.

measured in the scattering of thermal neutrons by electrons, then gives a mean square neutron radius

$$-\tfrac{1}{5}R_0{}^2 \simeq \langle r^2 \rangle_n = -\epsilon_n R_b{}^2 + \epsilon_n R_H{}^2 , \qquad (4.12)$$

which may be obtained by adjusting ϵ_n. For $R_b = R_0$ and $R_H = 8$ F, we find $\epsilon_n = -\tfrac{1}{5}\%$ of the proton's charge, and

$$G_{En} \cong (1/500)G_{Ep} \qquad (4.13)$$

for $q^2 > 0.3$ F^{-2}, which is consistent with the $G_{En} \simeq 0$ values obtained from electron-deuteron scattering.[31]

In any event, we note that the neutron, with $\langle r^2 \rangle_n \simeq -\tfrac{1}{5}R_0{}^2$ is smaller than the usual proton and is negligible compared with the proton halos we have been considering. Hence even a large neutron excess in heavy nuclei will not have a significant effect.

What are other consequences of a proton halo? We have calculated the contribution of the halo to other accurately measured level shifts. Since the mean square radius is additive, as in Eq. (4.9), we see that (except for a negligible contribution from the neutron) the Lamb shift in deuterium is increased by the same amount as in hydrogen. For other cases, we scale by $Z^4(2/n)^3$ and obtain the results listed in Table II. We note that in all cases except hydrogen and deuterium, the effect is smaller than the error limits and thus does not conflict with experiment.

We have also checked that the presence of a halo in the phosphorous nucleus does not disturb the precise determination of the muon mass from the $3D$-$2P$ muon x-ray transitions.[32]

The presence of nucleon halos also has negligible effect on the Coulomb contribution to the nucleon-nucleon scattering length and effective range.[33]

V. CONCLUSION

Although there are many theoretical objections to a proton charge distribution with a long tail,[34] the relevant experimental data do not rule out this possibility. On the contrary, the low momentum transfer electron-proton scattering data do seem to hint at such an effect. Our analysis of the muonic x rays of Bi^{209} gives a nuclear charge distribution with Fermi parameters at variance with that obtained from electron scattering; a nuclear halo resolves this discrepancy. A halo charge distribution on the neutron can fit the known features of the neutron charge form factor. Finally we note that a proton halo numerically consistent with

the above data implies a doubling of the proton mean square radius and brings the theory of the Lamb shift in H and D into good agreement with experiment. Thus in a *number* of different physical situations, discrepancies between theory and experiment of more than one standard deviation can each be interpreted in terms of a proton halo of radius $R_H \simeq 8$ F, and *positive* charge $\simeq 0.01$ e.

It should be noted that the above evidence (except for the electron-neutron interactions) could be interpreted alternatively in terms of a long charge tail on electrons and muons.[35]

We feel that the basic theory and analysis of the muon x rays given here is especially accurate due to our treatment of nuclear polarization, vacuum polarization, and the muonic Lamb shift, which we find to be as important as the dispersion contribution. The theory of electron-bismuth scattering, however, may need further refinement, especially in the treatment of the dispersion corrections.[36] Accurate low-energy scattering experiments on isotopically pure lead would be desirable.

Finally, we should emphasize that our interpretation of both the neutron and proton form factors depends on the acceptance of the data usually quoted. Data reduction for these quantities at low q^2 may have introduced additional systematic errors from radiative corrections, etc.[37] In the last analysis, however, the most direct determination of the existence of a nucleon halo would be given by the accurate measurement of the proton and neutron form factors at lower values of momentum transfer and better accuracy than heretofore obtained.

APPENDIX A: LAMB SHIFT IN HEAVY MUONIC ATOMS

For the second-order Lamb shift in light hydrogenic (i.e., one-lepton) atoms, the usual expansions[17] in powers of the field strength $\mathcal{E} = Z\alpha/r^2$ work well because $Z\alpha$ is very small. The expansion parameter is effectively $\pi Z\alpha$ for point nuclei for which integrals of singular operators such as $\mathcal{E}^2 = (Z\alpha)^2/r^4$ obtain their predominant contribution at distances r of the order of the Compton wavelength of the lepton. Such an expansion is thus questionable for determining the energy shift of the K shell in atomic mercury[16] or bismuth where $\pi Z\alpha \simeq 2$. In heavy *muonic* atoms, however, the Compton wavelength of the muon, $\lambda_\mu \simeq 2$ F, is smaller than the nuclear radius $R \simeq 7$ F, so the field strength becomes finite (owing to the finite extent of the nuclear charge distribution) somewhat before the relativistic region $r \sim \lambda_\mu$ is reached. The relevant expansion parameter is thus not $\pi Z\alpha$, but, say,

$$\frac{p}{m_\mu} \simeq \frac{1/R}{m_\mu} = \frac{\lambda_\mu}{R} \simeq 30\%.$$

[32] A. Petermann and Y. Yamaguchi, Phys. Rev. Letters **2**, 359 (1959); G. Feinberg and L. Lederman, Ann. Rev. Nucl. Sci. **13**, 441 (1963).

[33] We wish to thank H. Lipinski for the computer programs used for this analysis.

[34] In analogy with the usual explanation of nucleon form factors, a halo radius of 8 F would seem to imply the existence of low-mass ($\lesssim 100$ MeV) particles which *probably* would interact with known particles sufficiently strongly to have been detected heretofore. On the other hand, the smallness of $\epsilon \sim 1\%$ could indicate anomalous two-photon interactions with the proton.

[35] S. D. Drell (private communication).

[36] See Sec. III.

[37] L. N. Hand (private communication).

Evaluation of the leading higher-order term

$$\frac{2\alpha}{3\pi m}\langle \mathscr{E}^2\rangle \int_0^1 \frac{dz}{zm^2+(1-z)p^2}, \qquad (A1)$$

where $p\sim 1/R$, yields results 25% of the lowest-order contribution for the $1S$ state. These may be good estimates of the higher-order contributions, but we shall not include them because our estimates of the lowest-order contributions are only good to 30%.

To evaluate the lowest-order contribution Eq. (2.5), we need to evaluate or approximate the average excitation energy $\Delta\epsilon_n$ in the sum-over-states definition of the Bethe logarithm,[38]

$$\ln\frac{m}{2\Delta\epsilon_n}$$

$$\equiv \frac{\sum_{n'} \langle n|\mathbf{p}|n'\rangle\cdot\langle n'|[V,\mathbf{p}]|n\rangle \ln(m/2|E_n-E_{n'}|)}{\frac{1}{2}\langle n|\nabla^2 V|n\rangle}. \qquad (A2)$$

For a *point* Coulomb potential, the sum contains many continuum states $|n'\rangle$ with momenta of the order of $Z\alpha m$, and for the $1S$ state one finds a value of $\Delta\epsilon_n$ $\simeq 8(Z\alpha)^2 m$ which is large compared with E_n. However, for a finite charge distribution of extent $R\gg 1/Z\alpha m$, the electric field in the matrix element

$$\langle n'|[V,\mathbf{p}]|n\rangle \propto \int d^3r\, e^{i\mathbf{k}\cdot\mathbf{r}}\mathscr{E}(r)\phi_n(r) \qquad (A3)$$

will limit the contributing continuum states to those with momenta

$$k' \lesssim 1/R$$

and energies

$$E_{n'} = k'^2/2m \lesssim 1/2mR^2 = \frac{1}{2}(\lambda/R)^2 m/2.$$

For muonic bismuth, $E_{n'}\lesssim 4$ MeV, $E_{1S}=-10$ MeV, and the smallest excitation energy for the ground state is $E_{2P}-E_{1S}=6$ MeV, so the mean value theorem gives the range

$$|E_2-E_1| \leq \Delta\epsilon_1 \lesssim |E_1| + (E_{n'})_{\max}$$

or

$$6\text{ MeV} \lesssim \Delta\epsilon_1 \lesssim 14\text{ MeV};$$

therefore,

$$\ln\frac{m_\mu}{2\Delta\epsilon_1} \simeq \ln\frac{106\text{ MeV}}{2(10\pm4)\text{ MeV}} \simeq 1.7\pm0.4. \qquad (A4a)$$

Assuming that the average excitation energy level might also be at $E\simeq 0$ for the other states, we will take $\Delta\epsilon_n\simeq E_n$ to within a factor of 2. Since we are taking a logarithm, this sort of uncertainty does not introduce

---

[38] H. A. Bethe, Phys. Rev. **72**, 339 (1947).

TABLE IV. Expectation values of the functions X (energies in keV, lengths in F).

X	$1S_{1/2}$	$2S_{1/2}$	$2P_{1/2}$	$2P_{3/2}$	$3D_{3/2}$	$3D_{5/2}$	$4F_{5/2}$	$4F_{7/2}$	$5G_{7/2}$	$5G_{9/2}$
$1/r^2$	4.434×10^{-2}	1.037×10^{-2}	9.467×10^{-3}	7.647×10^{-3}	1.798×10^{-3}	1.632×10^{-3}	5.021×10^{-4}	4.841×10^{-4}	1.939×10^{-4}	1.907×10^{-4}
$1/r$	1.651×10^{-1}	6.111×10^{-2}	8.262×10^{-2}	7.708×10^{-2}	3.833×10^{-2}	3.684×10^{-2}	2.089×10^{-2}	2.056×10^{-2}	1.319×10^{-2}	1.310×10^{-2}
r	8.157	2.407×10^{1}	1.519×10^{1}	1.594×10^{1}	3.078×10^{1}	3.174×10^{1}	5.409×10^{1}	5.479×10^{1}	8.353×10^{1}	8.406×10^{1}
r^2	8.304×10^{1}	6.758×10^{2}	2.772×10^{2}	3.025×10^{2}	1.091×10^{3}	1.154×10^{3}	3.260×10^{3}	3.339×10^{3}	7.622×10^{3}	7.713×10^{3}
r^3	1.013×10^{3}	2.105×10^{4}	5.906×10^{3}	6.673×10^{3}	4.369×10^{4}	4.725×10^{4}	2.167×10^{5}	2.240×10^{5}	7.544×10^{5}	7.671×10^{5}
$-V/r^2$	9.933×10^{2}	2.170×10^{2}	1.492×10^{2}	1.075×10^{2}	1.285×10^{2}	1.074×10^{1}	1.704	1.595	3.851×10^{-1}	3.742×10^{-1}
$-V/r$	3.152×10^{2}	7.192×10^{2}	9.964×10^{2}	8.642×10^{2}	2.143×10^{2}	1.951×10^{2}	6.008×10^{1}	5.792×10^{1}	2.319×10^{1}	2.281×10^{1}
$-V$	1.606×10^{4}	6.478×10^{3}	9.567×10^{3}	9.057×10^{3}	4.585×10^{3}	4.409×10^{3}	2.499×10^{3}	2.460×10^{3}	1.578×10^{3}	1.566×10^{3}
$-Vr$	1.099×10^{5}	1.177×10^{5}	1.187×10^{5}	1.191×10^{5}	1.197×10^{5}	1.197×10^{5}	1.196×10^{5}	1.196×10^{5}	1.196×10^{5}	1.196×10^{5}
$-Vr^2$	9.442×10^{5}	2.875×10^{6}	1.815×10^{6}	1.907×10^{6}	3.684×10^{6}	3.799×10^{6}	6.469×10^{6}	6.553×10^{6}	9.986×10^{6}	1.005×10^{7}
$-Vr^3$	9.820×10^{6}	8.087×10^{7}	3.318×10^{7}	3.622×10^{7}	1.305×10^{8}	1.380×10^{8}	3.899×10^{8}	3.993×10^{8}	9.112×10^{8}	9.221×10^{8}
V^2	2.876×10^{8}	6.559×10^{7}	1.117×10^{8}	9.951×10^{7}	2.558×10^{7}	2.333×10^{7}	7.189×10^{6}	6.931×10^{6}	2.774×10^{6}	2.728×10^{6}
$(1/r)dV/dr$	3.282×10^{2}	5.242×10^{1}	1.152×10^{2}	9.966×10^{1}	1.305×10^{1}	1.098×10^{1}	1.704	1.593	3.846×10^{-1}	3.737×10^{-1}
$(dV/dr)^2$	6.253×10^{6}	7.620×10^{5}	2.177×10^{6}	1.860×10^{6}	1.400×10^{5}	1.053×10^{5}	7.219×10^{3}	6.380×10^{3}	8.774×10^{2}	8.381×10^{2}
$\rho_N(r)/\rho_N(0)$	4.095×10^{-1}	7.086×10^{-2}	7.621×10^{-2}	5.726×10^{-2}	1.924×10^{-7}	1.073×10^{-8}	9.289×10^{-6}	4.258×10^{-8}	1.701×10^{-8}	6.566×10^{-9}

large errors. Thus

$$\ln\frac{m}{2\Delta\epsilon_{2P}}\simeq \ln(53/4)\pm \ln2\simeq 2.5\pm 0.7 \qquad \text{(A4b)}$$

and

$$\ln\frac{m}{2\Delta\epsilon_{3D}}\simeq \ln(53/1.6)\simeq 3.5. \qquad \text{(A4c)}$$

The error limits in Eq. (2.7) include these uncertainties plus roughly 20% for higher-order terms.

In Table IV, we have tabulated the average values

$$\langle X\rangle \equiv \int_0^\infty dr(f^2+g^2)X \Big/ \int_0^\infty dr(f^2+g^2) \qquad \text{(A5)}$$

of various quantities X, where f/r and g/r are the large and small components of the numerical Dirac wave functions for the muon in the charge distribution Eq. (3.1), with $c=6.68$ F and $t=2.25$ F for Bi^{209}.

APPENDIX B: RESTRICTIONS FROM ELECTRON-PROTON SCATTERING

In order to provide a rough quantitative limitation on the halo from electron-proton scattering, let us restrict the value of the total form factor

$$G(q^2)=(1-\epsilon)G_b(q^2)+\epsilon G_H(q^2) \qquad \text{(B1)}$$

to lie within 3 standard deviations of Drickey and Hand's[39] value 0.9731 ± 0.0054 at $q^2=0.300$ F^{-2}, since this is the data point farthest from a smooth curve which passes through the other data and rises to a large value of $(1-G)/q^2$ at $q^2=0$. The 10 F halo shown in Fig. 1 is at the limit of this restriction.

For very large R_H, we have $G_H\simeq0$, and the restriction reduces to $\epsilon\leq1.1\%$, taking $R_b\simeq R_0$. This is the

same bound as would be obtained in a G versus q^2 plot by lowering the usual straight line parallel to itself until it was 3 standard deviations from the Drickey and Hand datum at $q^2=0.3$ F^{-2} and passed through $1-\epsilon_{\max}$ at $q^2=0$. We might note here that present $e\text{-}p$ scattering will not yield a smaller bound on ϵ than about 1% since this is the best accuracy (to date) of the form factor measurements.

For smaller R_H, we will (as we did in the hfs discussion) take the halo to be the same shape as the usual proton fit,

$$G_0(q^2)=(1+q^2R_0^2/12)^{-2} \qquad \text{(B2)}$$

but larger in spatial extent:

$$G_H(q^2)=(1+q^2R_H^2/12)^{-2}; \qquad \text{(B3)}$$

this corresponds to a charge density proportional to $e^{-(2\sqrt{3})r/R_H}$. The maximum value of ϵ allowed by the restriction is given as a function of R_H in Fig. 2. This upper bound is found to be decreased for halo shapes with more charge at large distances (such as a charge shell at $r=R_H$) and increased for halo shapes with more charge at small distances (such as a charge density proportional to $r^{-2}e^{-\sqrt{2}r/R_H}$). We will take the upper curve as the weakest bound since it lies above the curves for all the other halo shapes considered.

As we have noted before, taking the reduced body smaller than the usual proton will weaken the halo restrictions, raising the curves in Fig. 2. In order to limit the body size, let us consider the form factor Eq. (B1) at large q^2, where ϵG_H will be negligible. The form factor Eq. (B2) is within 15% of the data[40] and $\epsilon<5\%$, so G_b should agree with G_0 within 20%. For very large q^2, G scales roughly as $1/q^4R^4$, so we want $R_b\simeq R_0$ to within 5%. Therefore, we can safely state that the reduced body will raise the curves in Fig. 2 by less than half the amount shown for $R_b=0.9\ R_0$.

[39] D. J. Drickey and L. N. Hand, Phys. Rev. Letters **9**, 521 (1962).

[40] M. Goitein et al., Phys. Rev. Letters **18**, 1016 (1967), W. Albrecht et al., ibid. **18**, 1014 (1967).